The stereochemistry of overcrowded homomerous bistricyclic aromatic enes with alkylidene bridges

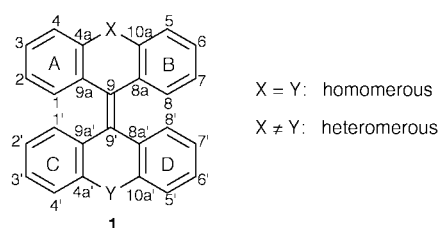**Yitzhak Tapuhi,† Michal Rachel Suissa,‡ Shmuel Cohen, P. Ulrich Biedermann, Amalia Levy and Israel Agranat ***

Department of Organic Chemistry, The Hebrew University of Jerusalem, Jerusalem 91904, Israel

The objective of the research was to study the effects of alkylidene bridges on the conformations and the conformational behaviour of overcrowded homomerous bistricyclic aromatic ethenes (**1**). The isopropylidene-bridged bistricyclic ethene **2** and **3** were synthesized by a reductive "dimerization" of **7**, using $TiCl_4$–Zn–pyridine–THF. The methylene-bridged bistricyclic ethenes **4–6** were synthesized by $LiAlH_4$–$AlCl_3$–Et_2O reductions of the corresponding bianthrones. The structures of **2–6** were established by ^1H- and ^{13}C-NMR spectroscopy and in the cases of **2** and **3**, also by X-ray analysis. Compounds **2** and **3** adopted C_i-*anti*-folded conformations with 53.0° and 28.8° folding dihedrals between pairs of benzene rings of tricyclic moieties. The central $C_9=C_{9'}$ bond in **2** was essentially planar. A short $C_9 \cdots C_{10}$ distance of 2.81 Å in **2** indicated an intramolecular overcrowding effect in the highly folded bistricyclic ethene. Semiempirical PM3 and AM1 calculations of the *anti*-folded, *syn*-folded, twisted and orthogonally twisted conformations of **2** and **4** indicated that *anti*-folded **2** and **4** were the most stable conformations with folding dihedrals of 48.7° and 45.0°, respectively at AM1. A DNMR spectroscopic study of *E*, *Z*-isomerizations and conformational inversions gave $\Delta G_c^{\ddagger}(E{\rightleftharpoons}Z) = 99.6$ kJ mol^{-1} ($CDBr_3$) and $\Delta G_c^{\#}$ (inversion) = 97.9 kJ mol^{-1} (hexachlorobutadiene) in **5** and $\Delta G_c^{\ddagger}$ (inversion) > 108 kJ mol^{-1} (benzophenone) in **3**. These high energy barriers were interpreted in terms of less overcrowded fjord regions in the *anti*-folded ground-state conformations.

Introduction

Bistricyclic aromatic enes (**1**) have served as attractive sub-
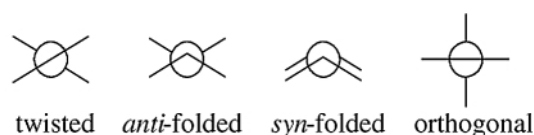

Fig. 1 Schematic projection along $C_9=C_{9'}$ of various types of conformations of bistricyclic enes (lines represent the peripheral benzene rings of the tricyclic moieties).

strates for the study of the conformations and dynamic stereochemistry of overcrowded ethenes.[1–3] Several of these systems, *e.g.*, bianthrone (**1**, X = Y: C=O) and dixanthylene (**1**, X = Y: O), display thermochromic, photochromic and piezochromic properties.[3] The bistricyclic enes are nonplanar due to the intramolecular overcrowding in their fjord regions.[3] The non-planarity introduces the notion of chirality to the arena of these interesting compounds.[4] Two principal modes of out-of-plane deviation were considered: twisting around the central carbon–carbon double bond and out-of-plane bending.[5] In **1**, the bending is realized by folding of the tricyclic moieties at both ends of the central ene about the $C_9 \cdots X$ and $C_{9'} \cdots Y$ axes, resulting in boat conformations of the central rings. In addition, the atoms C_9 and $C_{9'}$ may be pyramidalized. Four pure conformations of **1** were considered: the twisted (**t**), the *anti*-folded (**a**), the *syn*-folded (**s**) and the orthogonally twisted (**t**$_\perp$) conformations (Fig. 1).[3] Homomerous bistricyclic enes (**1**,

X = Y) with five-membered and six-membered central rings adopt twisted conformations (**t**) and *anti*-folded (**a**) conformations, respectively.[3]

Bistricyclic enes may undergo the following fundamental dynamic processes:[3]

1. *E*,*Z*-isomerization (*e.g.*, $t_E{\rightleftharpoons}t_Z$, $a_E{\rightleftharpoons}a_Z$),
2. Conformational inversion, *e.g.*, inversion of the helicity in the twisted **1** ($t_P{\rightleftharpoons}t_M$) or inversion of the boat conformation in the central rings of folded **1**,
3. *syn*, *anti*-isomerization (**a**$\rightleftharpoons$**s**), *anti*, twisted-isomerization (**a**$\rightleftharpoons$**t**) and *syn*, twisted-isomerization (**s**$\rightleftharpoons$**t**).
4. Enantiomerization and racemization may also be considered in these processes.

The dynamic stereochemistry of bistricyclic enes **1** with central six-membered rings have been studied by Agranat *et al.*, and by Feringa *et al.*, using dynamic NMR (DNMR) and equilibration techniques, when one of the conformational isomers is available in a pure form.[3–9] The DNMR studies revealed low barriers for thermal *E*,*Z*-isomerization ($\Delta G_c^{\ddagger}$ = 75–115 kJ mol^{-1}).[3,6–10] The range of free energies of activation for thermal conformational inversion of bistricyclic enes with central six-membered rings was found to be similar. These remarkably low energy barriers were interpreted predominantly in terms of ground state destabilization due to steric strain and overcrowding.[3] It has been shown that the barriers depend on the bridges

X and Y, on the C–X and C–Y bond lengths, and on the C_{4a}–C_{10a} distances.[6]

The present article describes the syntheses, molecular and crystal structures, semiempirical calculations and DNMR study of homomerous bistricyclic enes with methylene and isopropylidene bridges (**1**, X = Y: CH_2 and **1**, X = Y: CMe_2). In these systems, the C_{sp^2}–C_{sp^3} bonds at the bridges (C_{4a}–C_{10} and C_{10}–C_{10a}) are expected to be longer than the corresponding C_{4a}–X and C_{4a}–Y in dixanthylene, N,N'-dimethylbiacridan and bianthrone.[3] The alkylidene-bridged **1** are thus expected to possess a higher degree of folding and to be less overcrowded in the fjord regions. Furthermore, the methylene and isopropylidene bridges contain *axial* and *equatorial* hydrogen atoms and methyl groups in the boat-shaped central six-membered rings, which in principle allow a determination of the inversion barriers of the parent bistricyclic enes. Heteromerous bistricyclic enes with one CMe_2 bridge have previously been studied.[11]

Synthesis

The following compounds were synthesized: 10-[10,10-dimethyl-9(10H)-anthracenylidene]-9,10-dihydro-9,9-dimethyl-anthracene (**2**), 10-[10,10-dimethyl-9(10H)-anthracenyl]-9,10-
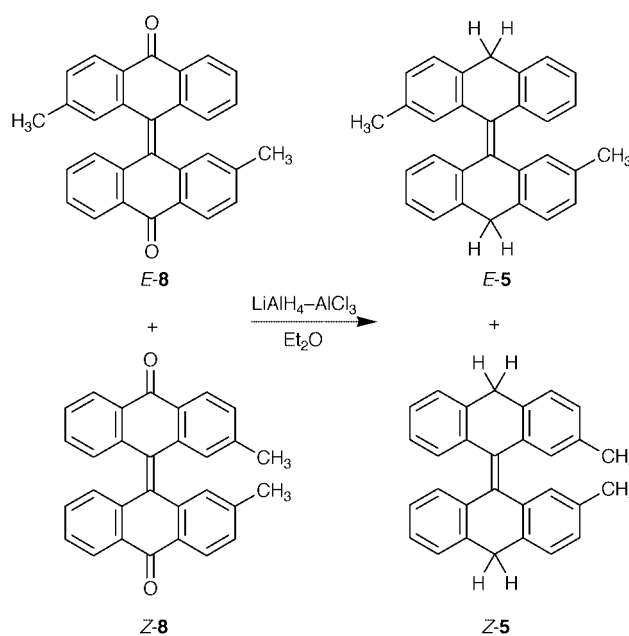

Scheme 1
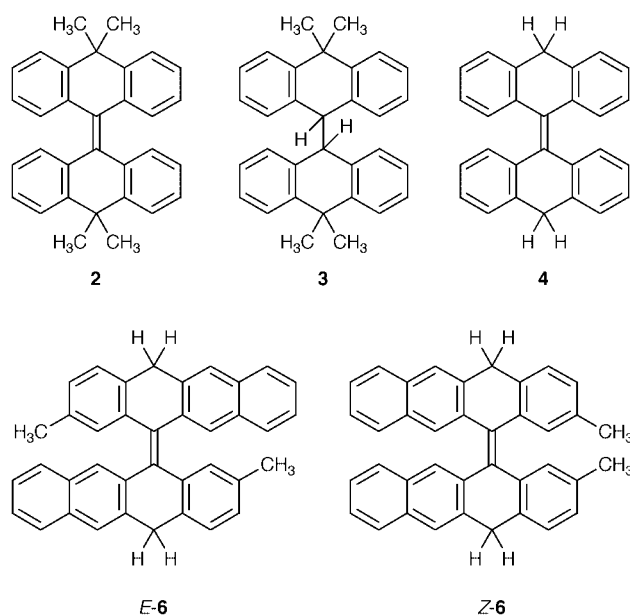
dihydro-9,9-dimethylanthracene (**3**), 9-[9(10H)-anthracenyl-idene]-9,10-dihydroanthracene (**4**), 9-[2-methyl-9(10H)-anthracenylidene]-9,10-dihydro-2-methylanthracene (**5**) and 5-[3-methyl-5(12H)-naphthacenylidene]-5,12-dihydro-3-methyl-naphthacene (**6**). The synthesis of **2** was accomplished by a low-valent titanium-induced reductive "dimerization" of 10,10-dimethylanthracen-9(10H)-one (**7**) using the Mukaiyama–Lenoir procedure[12–14] of the McMurry reaction[15] (TiCl$_4$–Zn–pyridine–THF) (Scheme 1). The reaction afforded a 1 : 3 mixture of **2** and **3** in 66% yield. The products were separated and purified by recrystallizations. Hydrocarbon **2** has been prepared by a reductive "dimerization" of **7**, using zinc in AcOH–HCl.[16] Hydrocarbon **3** has been prepared by hydrogenation of **2**, using sodium in pentan-1-ol.[16]

Compounds **4–6** were synthesized by LiAlH$_4$–AlCl$_3$ reduction of bianthrone, 2,2′-dimethylbianthrone and 12-[3-methyl-12-oxo-5(12H)-naphthacenylidene]-2-methylnaphthacen-5(12H)-one, respectively. The synthesis of **4** by a LiAlH$_4$ reduction of bianthrone[17] and by a reductive "dimerization" of anthrone using aluminium in CH$_3$CN under the irradiation of ultrasonic wave[18] has been reported. Compounds **5** and **6** were obtained as mixtures of *E*- and *Z*-diastereomers. The synthesis
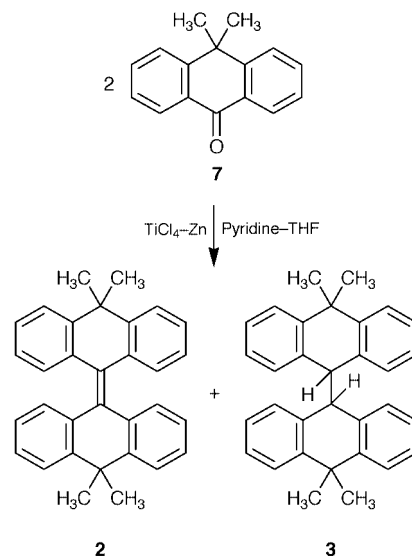
of (*E*)-**5** and (*Z*)-**5** is depicted in Scheme 2. The structures of **2**–**6** were established by NMR spectroscopy and elemental analysis. It is possible to distinguish qualitatively among the twisted, *syn*-folded and *anti*-folded conformations of homomerous bistricyclic enes (**1**, X = Y) in solution, using ¹H-NMR spectroscopy. In the cases of **2** and **4**, the fjord region protons appear at 7.010 and 6.984 ppm, respectively, indicating that these hydrocarbons adopt *anti*-folded conformations in solution.[3,8] A similar picture appears in **5** and **6**. In the case of **4**, complete assignments were made through two-dimensional correlation spectroscopy (COSY, HSQC, HMBC, NOESY). In the ¹H-NMR spectrum of **4**, the methylene protons appear as an AB system at 4.240 and 3.865 ppm. The doublet at 4.240 ppm representing one of the protons of each methylene group was broad, while the second doublet at 3.865 ppm representing the other proton of each methylene group was sharp. In the aromatic region, the double doublet at 7.365 ppm representing H$_4$, H$_5$, H$_{4'}$, H$_{5'}$ was also broad. A COSY experiment indicated an allylic coupling between the 7.365 ppm doublet and the 4.240 ppm doublet. A NOESY experiment indicated through space interactions between the 7.365 ppm doublet and the 3.865 ppm doublet. On the basis of these experiments, it is concluded
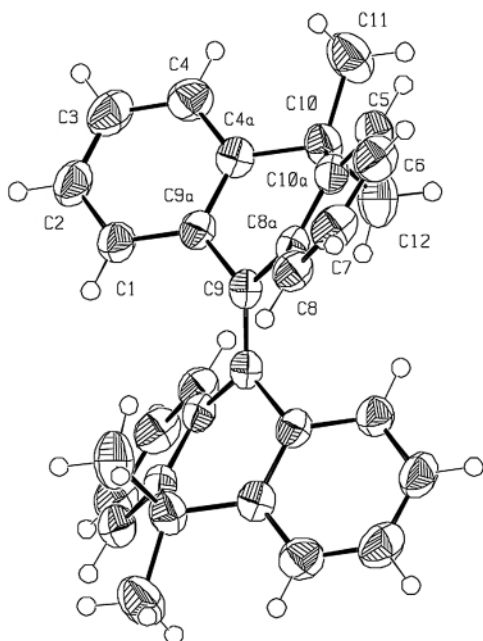
Fig. 2 An ORTEP drawing of **2** derived from the X-ray crystal structure.

that the 3.865 ppm doublet is due to the *equatorial* H_{10eq} while the 4.240 ppm doublet is due to the *axial* H_{10ax}.

Molecular and crystal structures §

Compounds **2** and **3** crystallized in the space group P2$_1$/*c*.[19] Fig. 2 gives an ORTEP diagram of one molecule of **2** as determined by X-ray analysis. Table 1 gives the conformations and selected geometrical parameters of **2–4** derived from the crystal structures and from semiempirical calculations (*vide infra*).

The molecular and crystal structures of **2** show that the molecule adopts a C_i-*anti*-folded conformation (**a-2**). The folding dihedral angle (between the least-squares-planes of the two benzene rings of each tricyclic moiety) of **2** is 53.0°. For comparison, the degree of folding of a metalo-based (PdCl$_2$ bridge) bistricyclic ene with the 9,9-dimethyl-9,10-dihydroanthracenylidene moiety is 48.8°.[11] The degree of overcrowding in the fjord regions of **2**, as reflected in the intramolecular distances $C_1 \cdots C_{1'}$, $C_1 \cdots H_{1'}$, and $H_1 \cdots H_{1'}$ is hardly significant: 3.13, 2.97 and 3.11 Å, respectively. For comparison, the van der Waals radii of carbon and hydrogen are 1.71 and 1.15 Å, resulting in van der Waals $C \cdots C$, $C \cdots H$ and $H \cdots H$ contact distances of 3.42 Å, 2.86 and 2.30 Å, respectively.[20] The above $C_1 \cdots C_{1'}$ distance in **2** reflects only an 8% penetration, while the above $C_1 \cdots H_{1'}$ and $H_1 \cdots H_{1'}$ distances do not indicate any penetration. On the other hand, the transannular $C_9 \cdots C_{10}$ distance, 2.81 Å is considerably shorter than the $C \cdots C$, van der Waals contact distance, reflecting an 18% penetration. These short distances indicate an additional effect of intramolecular overcrowding in highly folded bistricyclic enes.

In the previously reported structures of *anti*-folded homomerous bistricyclic enes, pyramidal $C_9=C_{9'}$ carbon atoms have been noted. However, the central carbon–carbon double bond in **2** is essentially planar, with negligible values of the pyramidalization angles χ_9 and $\chi_{9'}$,[3] and a pure twist of zero.[3] The $C_9=C_{9'}$ bond length is 1.347 Å. The relatively long C_{4a}–C_{10} bonds at the bridges, 1.534/1.531 Å, probably enhance the degree of folding. Overcrowding is also evident in the short contact distances between a methyl hydrogen and the corresponding *peri*-hydrogens (H$_4$, H$_5$): 2.16 Å.
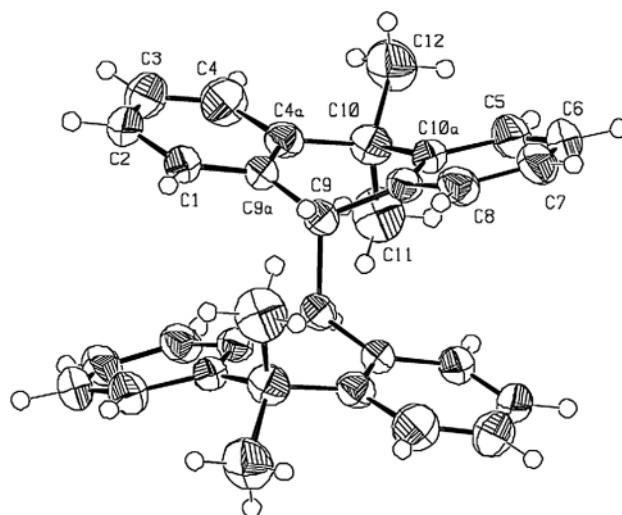
Fig. 3 An ORTEP drawing of **3** derived from the X-ray crystal structure.

Fig. 3 gives an ORTEP diagram of **3** as determined by X-ray analysis. The molecular and crystal structure of **3** show that the molecule adopts a C_i-*anti*-folded conformation. The folding dihedral angle (A–B, C–D) is 28.8°. The length of the central C_9–$C_{9'}$ is 1.587 Å. There is a certain degree of overcrowding: the $C_1 \cdots C_{1'}$ and $C_9 \cdots C_{10}$ distances are 3.07 and 2.97 Å, respectively. The short $H_4 \cdots H_3C$ distance, 2.04 Å should also be noted.

Semiempirical calculations

Recently, a systematic theoretical survey of overcrowded homomerous and heteromerous bistricyclic enes **1** has been carried out, using MOPAC 6.00 and the semiempirical method PM3.[3] The methylene- and isopropylidene-bridged bistricyclic enes **4** and **2** have been included, *inter alia*, in the modelling.[3] The present article reports the results of the PM3[21] and AM1[22] calculations of **4** and **2**, using MOPAC 93.[23] Comparisons of AM1 with PM3 have been commented on.[24,25] The following conformations of **2** and **4** have been considered: C_{2h}-*anti*-folded-**2** (**a-2**), C_{2v}-*syn*-folded-**2** (**s-2**), C_2-*syn*-folded-**2** (C_2-**s-2**), D_2-twisted-**2** (**t-2**), C_2-twisted-**2** (C_2-**t-2**), D_{2d}-orthogonally twisted-**2** (**t$_\perp$-2**), and the corresponding conformations of **4**, **a-4**, **s-4**, **t-4** and **t$_\perp$-4**. The various conformations have been fully optimized (Keywords: EF SYMMETRY PRECISE GNORM = 0.1 LET DDMIN = 0.0; for orthogonal conformations BIRADICAL was added) and their vibrational frequencies calculated (Keywords: FORCE PRECISE SYMMETRY; for orthogonal conformations BIRADICAL was added). The following conformations were found to be *bona fide* minima (positive vibrational frequencies): C_{2h}-**a-2**, C_2-**s-2**, C_2-**t-2**, C_{2h}-**a-4**, C_{2v}-**s-4** at PM3, C_{2h}-**a-2**, C_2-**s-2**, D_2-**t-2**, C_{2h}-**a-4**, C_{2v}-**s-4** at AM1. The following conformations were found to be transition states (one imaginary frequency): C_{2v}-**s-2**, D_2-**t-4** and D_{2d}-**t$_\perp$-4** at PM3, D_{2d}-**t$_\perp$-2**, D_2-**t-4** and D_{2d}-**t$_\perp$-4** at AM1. On the other hand, D_2-**t-2** at PM3 and C_{2v}-**s-2** at AM1 were found to be second order saddle points. Surprisingly, D_{2d}-**t$_\perp$-2** at PM3 was found to be a third order saddle point.

The semiempirical enthalpies of formation (ΔH_f°) of the conformations of **2** and **4**, the conformational energies ($\Delta\Delta H_f^\circ$) of **2** and **4** (relative to the respective *anti*-folded global minimum conformation) and selected geometrical parameters of the conformations of **2** and **4** derived from the PM3 and AM1 calculations are included in Table 1, together with the corresponding geometrical parameters derived from the crystal structures of **2** and **3**. The 3D structures of the AM1 optimized **s-2** and **a-4** are given in Fig. 4 and Fig. 5. The most stable conformations of **2** and **4** are the *anti*-folded conformations **a-2** and **a-4**. Their fold-

Table 1 Conformations, energies and geometrical parameters for compounds **2**–**4** derived from X-ray crystal structures and semiempirical calculations

Method	PG-Conf.[a]	ΔH_f°/ kJ mol⁻¹	$\Delta\Delta H_f^\circ$/ kJ mol⁻¹	Min/TS[b]	A–B/ deg	ω/deg	$C_9=C_{9'}$/Å	$C_{8a}–C_9–C_{9a}$/deg	$\chi(C_g)$/ deg	$C_{4a}–C_{10}$/ Å	$C_{10a}–C_{10}$/ Å	$C_{4a}–C_{10}–C_{10a}$/deg	$C_{4a}\cdots C_{10a}$/Å
Compound **2** C(CH₃)₂ bridges													
X-Ray	C_i-**a**				53.0	0.0	1.347(3)	110.2(1)	0.0(3)	1.533(2)	1.530(2)	106.7(1)	2.458(2)
PM3	C_{2h}-**a**	416.594	0.000	Min	45.2	0.0	1.352	110.8	4.0	1.517		108.9	2.47
AM1	C_{2h}-**a**	479.428	0.000	Min	48.7	0.0	1.355	111.0	1.5	1.512		107.9	2.45
PM3	C_2-**s**	430.574	13.979	Min	46.8	8.6	1.356	108.9	10.6	1.518	1.516	109.0	2.47
AM1	C_2-**s**	518.833	39.405	Min	50.7	24.7	1.357	109.6	9.5	1.516	1.511	107.9	2.45
PM3	C_{2v}-**s**	431.221	14.627	TS	46.3	0.0	1.356	108.7	10.3	1.517		109.2	2.47
AM1	C_{2v}-**s**	534.682	55.254	2	41.3	0.0	1.359	109.4	12.1	1.513		110.7	2.49
PM3	C_2-**t**	491.539	74.945	Min	9.4	53.2	1.394	117.4	−0.2	1.509	1.507	113.0	2.51
PM3	D_2-**t**	498.399	81.805	2	3.6	53.3	1.395	117.4	0.0	1.509		113.4	2.52
AM1	D_2-**t**	542.010	62.582	Min	5.2	51.5	1.393	117.3	0.0	1.504		113.4	2.51
PM3	D_{2d}-**t**$_\perp$	519.938	103.343	3	0.0	90.0	1.467	120.4	0.0	1.512		113.7	2.53
AM1	D_{2d}-**t**$_\perp$	568.715	89.287	TS	0.0	90.0	1.460	120.1	0.0	1.506		113.7	2.52
Compound **3** C(CH₃)₂ bridges													
X-Ray	C_i-**a**				28.7	0.0	1.585(4)	111.2(2)		1.536(3)	1.528(3)	110.8(2)	2.523(2)
Compound **4** CH₂ bridges													
PM3	C_{2h}-**a**	471.893	0.000	Min	47.9	0.0	1.352	110.9	3.5	1.496		109.7	2.45
AM1	C_{2h}-**a**	494.472	0.000	Min	45.0	0.0	1.356	111.7	2.7	1.491		110.4	2.45
PM3	C_{2v}-**s**	482.477	10.584	Min	52.2	0.0	1.350	109.5	13.0	1.497		109.0	2.44
AM1	C_{2v}-**s**	523.606	29.135	Min	50.1	0.0	1.353	109.9	14.9	1.494		109.9	2.44
PM3	D_2-**t**	545.962	74.069	TS	3.9	52.3	1.393	117.4	0.0	1.486		115.0	2.51
AM1	D_2-**t**	557.223	62.751	TS	4.3	50.9	1.392	117.4	0.0	1.483		115.0	2.50
PM3	D_{2d}-**t**$_\perp$	570.001	98.108	TS	0.0	90.0	1.466	120.3	0.0	1.488		115.2	2.51
AM1	D_{2d}-**t**$_\perp$	586.296	91.825	TS	0.0	90.0	1.459	120.1	0.0	1.485		115.3	2.51

Method	PG-Conf.[a]	$C_1\cdots C_{1'}$/Å	$C_1\cdots H_{1'}$/Å	$C_8\cdots H_{8'}$/Å	$H_1\cdots H_{1'}$/Å	$C_9\cdots C_{10}$/Å	$CH_3\cdots H_3C$/Å	$H_{10}\cdots H_{10'}$/Å	$C_9\cdots H_3C$/Å	$C_9\cdots H_{10}$/Å	$H_4\cdots H_3C$/Å	$H_5\cdots H_3C$/Å
Compound **2** C(CH₃)₂ bridges												
X-Ray	C_i-**a**	3.127(2)	2.98	2.95	3.11	2.811(2)	5.49		2.57		2.17	2.16
PM3	C_{2h}-**a**	3.06	2.96		3.24	2.84	5.80		2.76		1.87	
AM1	C_{2h}-**a**	2.99	2.83		3.07	2.82	5.44		2.57		2.03	
PM3	C_2-**s**	3.00	2.62	2.41	1.72	2.86	1.67		2.92		1.84	1.84
AM1	C_2-**s**	3.13	2.98	2.32	2.04	2.81	2.07		2.63		2.00	2.00
PM3	C_{2v}-**s**	2.99	2.51		1.71	2.87	1.64		2.97		1.83	
AM1	C_{2v}-**s**	2.97	2.59		1.85	2.89	1.81		3.13		1.93	
PM3	C_2-**t**	2.93	2.51	2.88	2.53	2.98	7.76		3.54		1.83	1.84
PM3	D_2-**t**	2.98	2.65		2.76	2.99	8.17		3.92		2.10	
AM1	D_2-**t**	2.91	2.59		2.72	2.99	8.09		3.90		2.12	
PM3	D_{2d}-**t**$_\perp$	3.78	3.49		3.53	2.95	8.47		3.88		2.17	
AM1	D_{2d}-**t**$_\perp$	3.78	3.49		3.53	2.95	8.44		3.87		2.14	
Compound **3** C(CH₃)₂ bridges												
X-Ray	C_i-**a**	3.070(4)	3.15	3.08	3.43	2.973(3)	6.24		2.26[c]		2.04	2.06
Compound **4** CH₂ bridges												
PM3	C_{2h}-**a**	3.07	2.93		3.19	2.80		3.26		3.06	2.42	
AM1	C_{2h}-**a**	2.94	2.77		3.02	2.82		3.24		3.11	2.41	
PM3	C_{2v}-**s**	3.06	2.55		1.74	2.77		3.29		2.98	2.42	
AM1	C_{2v}-**s**	3.10	2.69		1.94	2.76		3.28		2.99	2.42	
PM3	D_2-**t**	2.98	2.64		2.74	2.96		2.60		3.74	2.60	
AM1	D_2-**t**	2.91	2.58		2.69	2.96		2.61		3.75	2.61	
PM3	D_{2d}-**t**$_\perp$	3.81	3.52		3.56	2.92		2.65		3.69	2.65	
AM1	D_{2d}-**t**$_\perp$	3.81	3.52		3.56	2.92		2.66		3.71	2.66	

[a] Point group and conformation. [b] Minimum (Min), transition state (TS), or number of imaginary vibrational frequencies in case of a higher order saddle point. [c] $H_9\cdots H_3C$.

ing dihedrals are 48.7° and 45.0° at AM1, as compared with 53.0° in the crystal structures of **2**. In **a-2**, the $C_{4a}–C_{10}$ bond at the bridge is elongated, 1.517 Å (PM3) and 1.512 (AM1) as compared with **a-4**, 1.496 Å (PM3) and 1.491 Å (AM1).

In **a-2**, severe methyl, *peri*-H interactions are noted: the $CH_3\cdots H_4$ contact distance is 1.87 Å (PM3) and 2.03 Å (AM1). The short $CH_3\cdots C_9$ contact distance in **a-2** should also be noted: 2.76 Å (PM3) and 2.57 Å (AM1). These values are only slightly shorter than the van der Waals hydrogen···carbon contact distance (2.86 Å).[20] In **a-4**, the $C_9\cdots C_{10}$ dis-

tance, 2.84 Å (PM3) and 2.82 Å (AM1) reflects considerable penetration of the van der Waals carbon···carbon contact distance, 3.42 Å,[20] 17% (PM3) and 18% (AM1). The *anti*-folded conformations are only slightly pyramidalized. However, both *syn*-folded conformations are markedly pyramidalized at C_9: 10.6° (PM3) and 9.5° (AM1) in C_{2v}-**s-2** and 13.0° (PM3) and 14.9° (AM1) in **s-4**. The conformational energies of the *syn*-folded conformation are 14.0 (PM3) and 39.4 kJ mol⁻¹ (AM1) in C_2-**s-2** and 10.6 (PM3) and 29.1 kJ mol⁻¹ (AM1) in **s-4**. DFT *ab initio* calculations at B3LYP/6-31G*//HF/6-31G* on the

Table 2 Results of the ^{1}H DNMR studies of **5** and **6**

Compound	Solvent	Process	Probe	$\Delta\nu_c[H_2]$	T_c/K	$\Delta G_c^{\ddagger}$/kJ mol^{-1}
5	CDBr$_3$	$E \rightleftharpoons Z$	CH$_3$	3.75 ± 0.05^a	432 ± 5	99.6
6	1-C$_{10}$H$_7$Br	$E \rightleftharpoons Z$	CH$_3$	25 ± 1^b	467 ± 8	100.4
5	C$_4$Cl$_6$	Inversion	CH$_2$	41.2 ± 0.5^b	471 ± 8	97.9
6	1-C$_{10}$H$_7$Br	Inversion	CH$_2$	49 ± 1^b	465 ± 10	96.7

^{a} At 270 MHz. ^{b} At 100 MHz.
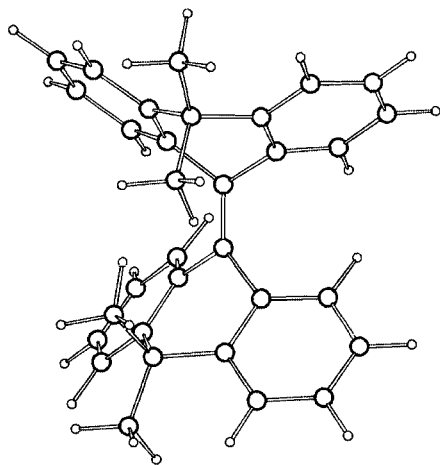
Fig. 4 3D structure of C_2-**s-2** calculated by AM1.
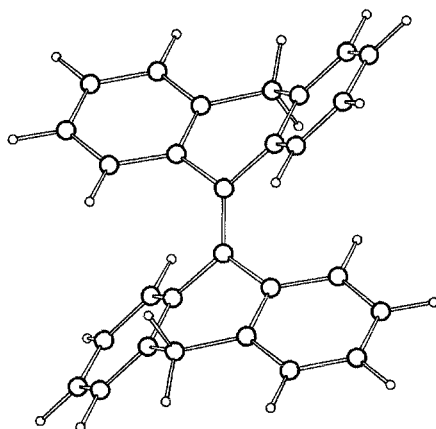
Fig. 5 3D structure of C_{2h}-**a-4** calculated by AM1.

related 10,10′-dimethylene derivative of **4** indicated that the *syn*-folded conformation is less stable than the *anti*-folded conformation by 39.1 kJ mol^{-1}.[26] The *syn*-folded conformations show also short $H_1 \cdots H_{1'}$ contact distances at the fjord regions (1.72 Å (PM3) and 2.04 Å (AM1) in C_2-**s-2** and 1.74 Å (PM3) and 1.94 Å (AM1) in **s-4**. In C_2-**s-2**, very short $CH_3 \cdots H_3C$ distances between the bridges are noted: 1.67 Å (PM3) and 2.07 Å (AM1). The conformational energies of the twisted conformations **t-2** and **t-4** are practically identical, 63 kJ mol^{-1} (AM1). The **a-4**→**s-4** photoisomerization and a CFF-π electron-CI calculation of **s-4** have been reported.[27,28]

DNMR Spectroscopy

The synthesis of **5** and **6** allowed a DNMR spectroscopic study of the conformational inversions and *E,Z*-isomerizations of these methylene-bridged bistricyclic enes. The ^{1}H-NMR spectrum of **5** included two methyl singlets, indicating the presence of the *E*- and *Z*-diastereomers. In an *anti*-folded conformation of **5**, the symmetries of the *E*- and *Z*-diastereomers are C_i and C_2 respectively; causing both methyl substituents in each diastereomer to be isochronous. The thermal *E,Z*-isomeriz-

ation was studied by monitoring the coalescence of the two methyl signals representing the *E*- and the *Z*-diastereomers, respectively. The conformational inversion of **5** and **6** was studied by monitoring the ^{1}H-NMR coalescence of the AB system representing the diastereotopic *axial* and *equatorial* hydrogens of the CH$_2$ bridges. It should be noted that in **5** and **6**, there was not any difference in the chemical shifts of the hydrogens of the CH$_2$ bridges between the *E*- and the *Z*-diastereomers. The results of the DNMR study are summarized in Table 2. In the case of **5**, $\Delta G_c^{\ddagger}$ ($E \rightleftharpoons Z$) = 99.6 kJ mol^{-1} (in CDBr$_3$) and $\Delta G_c^{\ddagger}$ (inversion) = 97.9 kJ mol^{-1} (in hexachlorobutadiene). In **6**, the corresponding $\Delta G_c^{\ddagger}$ values were 100.4 and 96.7 kJ mol^{-1} (in 1-bromonaphthalene). In the isopropylidene-bridged **2**, the ^{1}H-NMR and ^{13}C-NMR spectra led in each case to two separated singlets representing the *axial* and *equatorial* methyl groups. Upon a conformational inversion of **2**, a Me$_{ax}$⇌Me$_{eq}$ interconversion would be expected. A DNMR experiment in naphthalene ($\Delta\nu$ = 35 Hz) up to 207 °C did not show any significant broadening of the two ^{1}H NMR methyl singlets, indicating that $\Delta G_c^{\ddagger}$ > 92 kJ mol^{-1}. Likewise, in benzophenone ($\Delta\nu$ = 3 Hz) at 190 °C, the two methyl ^{1}H-NMR singlets could still be resolved indicating that $\Delta G_c^{\ddagger}$ > 108 kJ mol^{-1}. Feringa *et al.* have reported on the conformational inversion of a few cases of heteromerous bistricyclic enes with isopropylidene bridges.[6] As in the case of **2**, a DNMR study of metalo-bridged bistricyclic enes with CMe$_2$ and ZnCl$_2$ bridges and with CMe$_2$ and PdCl$_2$ bridges did not result in a coalescence of the methyl signals even at 200 °C (in nitrobenzene-d$_5$).[11] The authors suggested that in these cases the results indicated considerable steric hindrance for the isomerization process inverting the folded conformations, and that metal binding results in folded structures completely inert towards interconversions.[11] In the case of 9-[10,10-dimethyl-9(10H)-anthracenylidene]-2-methyl-9H-thioxanthene in which the bridges are CMe$_2$ and S, the racemization barrier $\Delta G_c^{\ddagger}$ = 105 ± 1 kJ mol^{-1}.[6]

Table 3 gives the free energies of activation for thermal *E,Z*-isomerizations and for thermal conformational inversions of various homomerous bistricyclic enes. The most remarkable result of the present DNMR studies is the relatively high and essentially identical values of the free energies of activation for the *E,Z*-isomerization and for the conformational inversion. These results are consistent with the mechanisms of the conformational processes of *anti*-folded bistricyclic enes depicted in Fig. 6 and 7.[3] These mechanisms involve a common "edge passage" highest transition state. The higher energy barriers observed in the cases of the methylene-bridged and isopropylidene-bridged bistricyclic enes (*e.g.*, **5** and **2**) as compared with dixanthylenes[8] and bianthrones[9] are primarily due to the less overcrowded fjord regions in the *anti*-folded ground states of these systems. The longer C–X bonds in **2**, **5** and **6** and the longer $C_{4a} \cdots C_{10a}$ bridge distance allow a higher degree of folding and thus a reduced overcrowding in the fjord regions.[6] Such an effect is more pronounced in the case of the isopropylidene-bridged **2** as compared with the methylene-bridged **4**. The significantly higher barrier for the conformational inversion of **2** *versus* **5** ($\Delta\Delta G_c^{\ddagger}$ > 8 kJ mol^{-1}e) may also be ascribed to unfavorable steric interactions between one of the methyl groups of **2** and the fjord regions at the opposing ring (*e.g.*, $CH_3 \cdots H_{1'}$) in the transition state, during the "edge passage".

Table 3 Free energies of activation for thermal E,Z-isomerizations and for conformational inversions of homomerous bistricyclic enes [3]

System $\mathbf{1}$, X = Y	$\Delta G^{\ddagger}$ ($E \rightleftharpoons Z$)/ kJ mol^{-1}	Substituent	$\Delta G^{\ddagger}$ (inversion)/ kJ mol^{-1}	Substituent
—	104.4	2,2'-di-CH$_3$	43.9	2-CH(CH$_3$)$_2$
O	73.2	2,2'-di-CH(CH$_3$)$_2$	74.1	2,2'-di-CH(CH$_3$)$_2$
C=O	83.7	2,2'-di-CH$_3$	87.9	2,2'-di-OCH(CH$_3$)$_2$
NCH$_3$	87.0	2,2'-di-CH$_3$	—	—
S	114.6	2-CH$_3$	114.6	2-CH$_3$
CH$_2$[a]	99.6	2,2'-di-CH$_3$	97.9	2,2'-di-CH$_3$
C(CH$_3$)$_2$[a]	—	—	108	—

[a] This work.
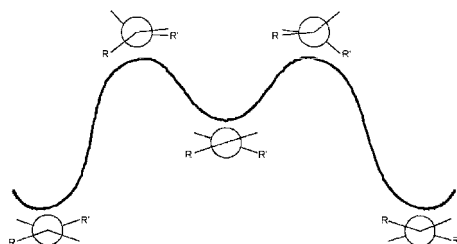
Fig. 6 Mechanism of the thermal conformational inversion of *anti*-folded bistricyclic enes.
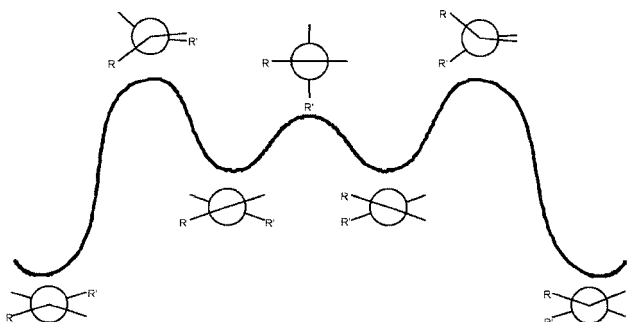
Fig. 7 Mechanism of the thermal E,Z-isomerization of *anti*-folded bistricyclic enes.

Experimental

Melting points are uncorrected. All NMR spectra were recorded with a Bruker DRX 400 spectrometer, unless otherwise stated. ^{1}H NMR spectra were recorded at 400.1 MHz using CDCl$_3$ as solvent and as internal standard (δ(CHCl$_3$) = 7.26 ppm). ^{13}C NMR spectra were recorded at 100.6 MHz using CDCl$_3$ as solvent and as internal standard (δ(CHCl$_3$) = 77.01 ppm). The barriers were determined by DNMR spectroscopy, substituting the coalescence temperature T_c and the extrapolated chemical shift difference $\Delta\nu_c$ at T_c in the following equation for the Eyring Equation $\Delta G_c^{\ddagger} = 4.47 \ T_c \ [9.97 - \log (T_c/\Delta\nu_c)]$.

10-[10,10-Dimethyl-9(10*H*)-anthracenylidene]-9,10-dihydro-9,9-dimethylanthracene (2) and 10-[10,10-dimethyl-9(10*H*)-anthracenyl]-9,10-dihydro-9,9-dimethylanthracene (3) [29]

The reaction was carried out under an argon atmosphere in a 500 mL three-necked round-bottomed flask equipped with a reflux condenser (protected from moisture), a dropping funnel, and a magnetic stirrer. Freshly distilled dry THF (200 mL) distilled over sodium diphenyl ketyl) was added to the flask and cooled to −5 °C. Dropwise slow injection of TiCl$_4$ (1.85 mL, 16.9 mmol) using a plastic syringe with continuous stirring gave a yellow complex, which was treated with Zn dust (2.26 g, 35.5 mmol). The temperature was gradually raised to rt and kept for another 1 h to give a greenish suspension. The mixture was then refluxed for 5 h to complete the reduction,

giving a green–black suspension. After cooling to 0 °C, the mixture was treated with pyridine (2 mL), followed by dropwise addition over 3.5 h of a solution of ketone **7** (3.50 g, 15.5 mmol)[22] in dry THF (100 mL). The resulting mixture was refluxed for 48 h. The disappearance of the starting material was monitored by TLC. After being cooled to room temperature, the mixture was added to dichloromethane (300 mL), stirred vigorously and treated with aqueous HCl (0.1 M) to give two layers. The organic layer was separated, and the aqueous layer was extracted with dichloromethane. The organic layers were dried (MgSO$_4$), and the solvents were removed in vacuum. The crude products (3.0 g) were dissolved in dichloromethane and chromatographed on a silica column, using a hexane–diethyl ether gradient (up to 20% diethyl ether) as eluent. The chromatography afforded 2.1 g (65.6% yield) of the fluorescent yellow products. The ^{1}H-NMR spectrum (*vide infra*) indicated a 1:3 mixture of **2** and **3**. Recrystallization from benzene gave single crystals of **2** (1:1 complex with benzene), mp 325 °C, suitable for X-ray analysis (lit.,[16] mp 312–313 °C).

Anal. Calcd for C$_{38}$H$_{34}$ (C$_{32}$H$_{28}$·C$_6$H$_6$): C, 93.02; H, 6.98. Found: C, 93.26; H, 6.87%. ^{1}H-NMR (300 MHz, CDCl$_3$ δ = 7.26 ppm) δ: 7.526 (br d, ^3J = 7.7 Hz, 4H, H$_4$, H$_5$, H$_{4'}$, H$_{5'}$), 7.153 (dt, ^3J = 7.5 Hz, ^4J = 1.5 Hz, 4H, H$_3$, H$_6$, H$_{3'}$, H$_{6'}$), 7.010 (dd, ^3J = 7.7 Hz, ^4J = 1.5 Hz, 4H, H$_1$, H$_8$, H$_{1'}$, H$_{8'}$), 6.885 (dt, ^3J = 7.4 Hz, ^4J = 1.0 Hz, 4H, H$_2$, H$_7$, H$_{2'}$, H$_{7'}$), 1.974 (s, 6H, CH$_3$), 1.851 (s, 6H, CH$_3$). ^{13}C-NMR (50.29 MHz, CDCl$_3$ δ = 77.008 ppm) δ 147.338, 137.885, 130.516, 128.851, 126.479, 124.572, 122.970, 40.438, 30.831, 24.257. MS (140 °C, % P) m/z 412 (C$_{32}$H$_{28}$$^{+\bullet}$, 97), 411 (C$_{32}H_{27}$$^{+\bullet}$, 100), 382 (C$_{30}H_{22}$$^{+\bullet}$, 98), 367 (C$_{29}H_{19}$$^{+\bullet}$, 17), 352 (C$_{28}H_{16}$$^{+\bullet}$, 25), 206 (C$_{16}H_{14}$$^{+\bullet}$, 15), 191 (C$_{30}H_{28}$$^{2+}$, 66), 176 (C$_{28}H_{16}$$^{2+}$, 89), 175 (C$_{28}H_{14}$$^{2+}$, 90).

Crystal data. Compound **2**: Formula C$_{32}$H$_{28}$·C$_6$H$_6$, M = 490.69, monoclinic, a = 9.658 (8), b = 15.375 (4), c = 9.975 (2) Å, β = 103.78 (5)°, V = 1438.6 (9) Å^3, rt, space group P2$_1$/c (no.14), Z = 2, μ(Mo-Kα) = 0.32 cm^{-1}, 2306 unique reflections of which 1823 were observed ($I > 2\sigma_I$), R = 0.033, R_w = 0.045.

Compound **3** was isolated from the filtrate of the recrystallization of **2**. The solvent was removed in vacuum and the remaining solid was recrystallized three times from dichloromethane. Sublimation at 170 °C/0.1 mmHg gave single crystals of **3**, mp 258 °C, suitable for X-ray analysis (lit.,[16] mp 260 °C).

Anal. Calcd for C$_{32}$H$_{30}$: C, 92.70; H, 7.30. Found: C, 92.42; H, 6.99%. ^{1}H-NMR (400 MHz, 363 K, Cl$_2$CDCDCl$_2$ δ = 5.15) δ 7.396 (d, ^3J = 8.0 Hz, 4H, H$_4$, H$_5$, H$_{4'}$, H$_{5'}$), 7.179 (t, ^3J = 7.1 Hz, 4H, H$_3$, H$_6$, H$_{3'}$, H$_{6'}$), 6.915 (t, ^3J = 7.5 Hz, 4H, H$_2$, H$_7$, H$_{2'}$, H$_{7'}$), 6.419 (br d, ^3J = 7.4 Hz, 4H, H$_1$, H$_8$, H$_{1'}$, H$_{8'}$), 4.440 (s, 2H, H$_9$, H$_{9'}$), 1.562 (s, 6H, CH$_3$), 0.971 (s, 6H, CH$_3$). ^{13}C-NMR (100 MHz, 363 K, Cl$_2$CDCDCl$_2$, δ = 77.007 ppm) δ: 145.71 (C$_{4a}$, C$_{10a}$, C$_{4a'}$, C$_{10a'}$), 135.19 (C$_{8a}$, C$_{9a}$, C$_{8a'}$, C$_{9a'}$), 129.75 (C$_1$, C$_8$, C$_{1'}$, C$_{8'}$), 126.92 (C$_3$, C$_6$, C$_{3'}$, C$_{6'}$), 126.35 (C$_4$, C$_5$, C$_{4'}$, C$_{5'}$), 125.27 (C$_2$, C$_7$, C$_{2'}$, C$_{7'}$), 55.78 (C$_9$, C$_{9'}$), 38.62 (C$_{10}$, C$_{10'}$), 33.85 (CH$_3$), 33.64 (CH$_3$). MS (150 °C, % P). m/z 208 (C$_{16}$H$_{16}$$^{+\bullet}$, 70), 207 (C$_{16}H_{15}$$^{+\bullet}$, 100), 193 (C$_{15}H_{13}$$^{+\bullet}$, 71), 192 (C$_{15}H_{12}$$^{+\bullet}$, 97), 191

$(C_{15}H_{11}^{+\bullet}$, 74), 190 $(C_{15}H_{10}^{+\bullet}$, 26), 189 $(C_{15}H_9^{+\bullet}$, 69), 178 $(C_{14}H_{10}^{+\bullet}$, 33), 165 $(C_{13}H_9^{+\bullet}$, 49).

Crystal data. Compound **3**: Formula $C_{32}H_{30}$, $M = 414.59$, monoclinic, $a = 12.139$ (4), $b = 8.260$ (3), $c = 11.816$ (3) Å, $\beta = 90.97$ (4)°, $V = 1184.6$ (7) Å^3, rt, space group $P2_1/c$ (no.14), $Z = 2$, μ(Mo-Kα) = 0.33 cm^{-1}, 2269 unique reflections of which 1553 were observed ($I > 2\sigma_I$), $R = 0.055$, $R_W = 0.068$.

9-[2-Methyl-9(10H)-anthracenylidene]-9,10-dihydro-2-methyl-anthracene (5)

The reaction was carried out in an argon atmosphere in a round-bottomed flask equipped with a reflux condenser (protected from moisture) and a magnetic stirrer. Dry diethyl ether (30 ml) was added to the flask followed by anhydrous AlCl$_3$ (3.6 g, 27 mmol) in small portions and then by LiAlH$_4$ (0.6 g, 15.8 mmol) in small portions. The mixture was stirred for 30 min at rt, dry benzene (50 ml) was added followed by 2,2′-dimethyl-bianthrone (**8**)[9] (0.25 g, 0.6 mmol) in small portions. The mixture was then refluxed at 80 °C for 3 h. The excess LiAlH$_4$ was decomposed by adding dropwise ethyl acetate and the mixture treated by water, followed by dilute aqueous HCl. The organic layer was separated and the aqueous layer extracted with dichloromethane. The combined organic layers were dried (MgSO$_4$), and the solvents were removed in vacuum. The crude product was purified by preparative chromatography on a PLC silica plate, using benzene as eluent ($R_f = 0.9$). Recrystallization from benzene–petrol ether (40–60 °C) gave **5** as a colorless powder, mp 265–272 °C, in 65% yield. The $E:Z$ ratio was 55:45 (or *vice versa*).

Anal. Calcd for $C_{30}H_{24}$: C, 93.70; H, 6.30. Found: C, 93.44; H, 6.08%. ^{1}H-NMR (400 MHz, CDCl$_3$, $\delta = 7.26$ ppm) 7.349 (d, $^3J = 7.5$ Hz, 2H), 7.247 (d, $^3J = 7.5$ Hz, 2H), 7.076–7.122 (t, $^3J = 7.4$ Hz, $^4J = 1.5$ Hz, 2H), 6.912–6.975 (m, 4H), 6.877 (t, $^3J = 7.4$ Hz, 2H), 6.787 (br s, 0.45 × 2H), 6.759 (br s, 0.55 × 2H), 4.214 (br d, $J = 16.2$ Hz, 2H), 3.827 (sd, $J = 16.2$ Hz, 2H), 2.052 (s, 0.45 × 6H CH$_3$), 2.037 (s, 0.55 × 6H, CH$_3$). δ (CH$_3$) $\nu_E - \nu_Z$ (270 MHz, CDBr$_3$, CH$_3$ signals) 3.75 Hz. $\Delta\delta$ (CH$_2$, AB system) 100 MHz, hexachlorobutadiene). $\nu_A - \nu_B = 41.2$ Hz, $^2J = 16.3$ Hz. DNMR (270 MHz), CDBr$_3$, $T_c = 4.32 \pm 5$ K, $\Delta\nu_c = 3.75 \pm 0.05$ Hz, (CH$_3$), $\Delta G_c^{\ddagger}$ ($E\rightleftharpoons Z$) = 99.6 kJ mol^{-1}. DNMR (100 MHz), hexachlorobutadiene, $T_c = 471 \pm 8$ K, $\Delta\nu_c = 41.2 \pm 0.5$ (CH$_2$), $\Delta G_c^{\ddagger}$ (inversion) = 97.9 kJ mol^{-1}. MS (% P) m/z: 385 ($^{13}C^{12}C_{29}H_{24}^{+\bullet}$, 32), 384 ($^{12}C_{30}H_{24}^{+\bullet}$, 100), 383 ($^{12}C_{30}H_{23}$, 26), 382 ($^{12}C_{30}H_{22}^{+\bullet}$, 45), 192 ($^{12}C_{30}H_{24}^{+2}$, 73). UV (CH$_2Cl_2$) λ_{max} nm (log ε): 253 (4.24), 323 (4.13). ^{13}C-NMR (100 MHz, CDCl$_3$) δ: 139.24, 139.12, 137.90, 137.77, 137.56, 137.39, 135.99, 135.87, 134.14, 133.05, 131.84, 129.63, 129.57, 129.02, 128.93, 127.04, 126.80, 126.65, 126.63, 126.28, 126.26, 124.76, 124.55, 37.15 (C$_{10'}$, C$_{10'}$), 37.14 (C$_{10'}$, C$_{10'}$), 20.95 (CH$_3$), 20.85 (CH$_3$).

9-[9(10H)-Anthracenylidene]-9,10-dihydroanthracene (4)

Hydrocarbon **4** was prepared by a LiAlH$_4$–AlCl$_3$ reduction of bianthrone (**1**, X = Y: C=O) analogously to **5** in 50% yield and was obtained after recrystallization from toluene as colorless powder, mp 288–291 °C (decomp.). (Lit.,[17] mp 328 °C).

Anal. Calcd for $C_{28}H_{20}$: C, 94.34; H, 5.66. Found: C, 94.75; H, 5.76%. ^{1}H-NMR (400 MHz, CDCl$_3$) δ: 7.364 (dd, $^3J = 7.5$ Hz, 4H, H$_4$, H$_5$, H$_{4'}$, H$_{5'}$), 7.117 (dt, $^3J = 7.4$ Hz, $^4J = 1.4$ Hz, 4H, H$_3$, H$_6$, H$_{3'}$, H$_{6'}$), 6.984 (dd, $^3J = 7.8$, $^4J = 1.0$ Hz, 4H, H$_1$, H$_8$, H$_{1'}$, H$_{8'}$), 6.894 (dt, $^3J = 7.5$ Hz, $^4J = 1.1$ Hz, 4H, H$_2$, H$_7$, H$_{2'}$, H$_{7'}$), 4.240 (br d, $^2J = 16.2$ Hz, 2H, CH$_2$), 3.865 (d, $J = 15.8$ Hz, 2H, CH$_2$). ^{13}C-NMR (100 MHz, CDCl$_3$) δ 37.60 (CH$_2$, C$_{10}$, C$_{10'}$), 124.83 (C$_2$, C$_7$, C$_{2'}$, C$_{7'}$), 126.39 (C$_3$, C$_6$, C$_{3'}$, C$_{6'}$), 128.96 (C$_1$, C$_8$, C$_{1'}$, C$_{8'}$), 131.97 (C$_9$, C$_{9'}$), 137.70 (C$_{8a}$, C$_{9a}$, C$_{8a'}$, C$_{9a'}$), 139.06 (C$_{4a}$, C$_{10a}$, C$_{4a'}$, C$_{10a'}$). MS (% P) m/z 357 ($^{13}C^{12}C_{27}H_{20}^{+\bullet}$, 32), 356 ($^{12}C_{28}H_{20}^{+\bullet}$, 100), 355 ($^{12}C_{28}H_{19}^{+\bullet}$, 20), 354 ($^{12}C_{28}H_{18}$, 12), 179 (36), 178 ($^{12}C_{30}H_{20}^{+2}$, 96). UV (CH$_2Cl_2$) λ_{max} nm (log ε): 253 (4.34), 320 (4.20).

5-[3-Methyl-5(12H)-naphthacenylidene]-5,12-dihydro-3-methylnaphthacene (6)

Hydrocarbon **6** was prepared by a LiAlH$_4$–AlCl$_3$ reduction of 2-methyl-12-[3-methyl-12-oxo-5(12H)-naphthacenylidene]-naphthacen-5(12H)-one,[9] analogously to **4**. The product was purified on a silica PLC plate, using dichloromethane–petrol ether (40–60 °C) 1:1 as eluent ($R_f = 0.7$). Recrystallization from benzene–petrol ether (40–60 °C) gave **6** as a pale yellowish powder, mp >300 °C (slow decomposition during heating to give a brown–red color). The yield was 72%. The $E:Z$ ratio was 52:48 (or *vice versa*).

Anal. Calcd for $C_{38}H_{28}$: C, 94.18; H, 5.82. Found: C, 94.33; H, 5.99%. ^{1}H-NMR (400 MHz, CDCl$_3$) δ: 1.834 (s, 0.52 × 6H, (CH$_3$)$_2$), 2.059 (s, 0.48 × 6H, (CH$_3$)$_2$), 4.061 (d, $^2J = 15.9$, 2H, H$_{10}$, H$_{10'}$), 4.451* (br d, $^2J = 16.0$, 2H, H$_{10}$, H$_{10'}$), 6.784 (br s, 0.52 × 2H), 6.809 (br s, 0.48 × 2H), 6.914 (d, $^3J = 7.6$, $^4J = 1.0$, 0.52 × 2H), 6.960 (d, $^3J = 7.5$, $^4J = 0.8$, 0.48 × 2H), 7.136 (t, $^3J = 7.9$, $^4J = 1.1$, 0.52 × 2H), 7.209 (d, $^3J = 8.1$, 0.52 × 2H), 7.278–7.346 (m, 5.8H), 7.386 (t, $^3J = 8.0$, $^3J = 6.8$, $^4J = 1.3$, 0.52 × 2H), 7.432 (d, $J = 8.1$ Hz, 0.52 × 2H), 7.489 (s, 2H), 7.751 (t, 2H), 7.838 (d, $J = 7.9$, 2H). DNMR (100 MHz), 1-bromonaphthalene, $T_c = 4.67 \pm 8$ K, $\Delta\nu_c = 25 \pm 1$ Hz, (CH$_3$), $\Delta G_c^{\ddagger}$ ($E\rightleftharpoons Z$) = 100.4 kJ mol^{-1}; $T_c = 465 \pm 10$ K, $\Delta\nu_c = 49 \pm 1$ (CH$_2$), $\Delta G_c^{\ddagger}$ (inversion) = 96.7 kJ mol^{-1}. ^{13}C-NMR (100 MHz, CDCl$_3$) δ: 20.85 (CH$_3$), 20.89 (CH$_3$), 37.45 (C$_{10}$, C$_{10'}$), 37.48 (C$_{10}$, C$_{10'}$), 124.60, 124.86, 124.89, 124.98, 125.69, 125.73, 126.62, 126.77, 126.86, 126.87, 127.33, 127.34, 127.48, 127.78, 127.84, 127.92, 129.32, 129.59, 131.44, 131.50, 132.10, 132.10, 132.18, 132.71, 132.75, 134.24, 134.51, 135.89, 135.91, 135.92, 135.94, 137.29, 137.32, 137.43, 137.51. MS (% P) m/z: 485 ($^{13}C^{12}C_{37}H_{28}^{+\bullet}$, 42), 484 ($^{12}C_{38}H_{28}^{+\bullet}$, 100), 483 (10), 482 (9), 469 ($^{12}C_{37}H_{25}^{+\bullet}$, 5), 242 ($^{12}C_{38}H_{28}^{+2}$, 30). UV (CH$_2Cl_2$) λ_{max} nm (log ε): 237 (4.19), 275 (3.81), 348 (3.38).

References

1 G. Shoham, S. Cohen, R. M. Suissa and I. Agranat, in *Molecular Structure: Chemical Reactivity and Biological Activity*, eds. J. J. Stezowski, J.-L. Huang and M.-C. Shao, Oxford University Press, Oxford, 1988, p. 290.
2 J. Sandström, in *The Chemistry of Double-Bonded Functional Groups, Supplement A3*, ed. S. Patai, Wiley, New York, 1997, p. 1253.
3 P. U. Biedermann, J. J. Stezowski and I. Agranat, in *Advances in Theoretically Interesting Molecules*, Vol. 4, ed. R. P. Thummel, JAI Press, Stamford, CT, 1998, p. 245.
4 P. U. Biedermann, A. Levy, J. J. Stezowski and I. Agranat, *Chirality*, 1995, **7**, 199.
5 A. Z.-Q. Khan and J. Sandström, *J. Am. Chem. Soc.*, 1988, **110**, 4843.
6 B. L. Feringa, W. F. Jager and B. de Lange, *Tetrahedron Lett.*, 1992, **33**, 2887.
7 I. Agranat and Y. Tapuhi, *J. Am. Chem. Soc.*, 1978, **100**, 5604.
8 I. Agranat and Y. Tapuhi, *J. Am. Chem. Soc.*, 1979, **101**, 665.
9 I. Agranat and Y. Tapuhi, *J. Org. Chem.*, 1979, **44**, 1941.
10 I. O. Sutherland, *Annu. Rep. N.M.R. Spectrosc.*, 1971, **4**, 71.
11 (*a*) W. I. Smid, A. M. Schoevaars, W. Kruizinga, N. Veldman, W. J. J. Smeets, A. L. Spek and B. L. Feringa, *Chem. Commun.*, 1996, 2265; (*b*) 3D Search and Research Using the Cambridge Structural Database, F. H. Allen and O. Kennard, *Chem. Design Autom. News*, 1993, **8**(1), 31.
12 T. Mukaiyama, T. Sato and J. Hanna, *Chem. Lett.*, 1973, 1041.
13 D. Lenoir and P. Lemmen, *Chem. Ber.*, 1980, **113**, 3112.
14 I. Agranat, S. Cohen, R. Isaksson, J. Sandström and M. R. Suissa, *J. Org. Chem.*, 1990, **55**, 4943.
15 J. March, *Advanced Organic Chemistry: Reactions, Mechanisms and Structure*, 4th edn., Wiley, New York, 1992, p. 1227.
16 C. Herberg, H.-D. Beckhaus and C. Rüchardt, *Chem. Ber.*, 1994, **127**, 2065.
17 A. F. A. Ismail and Z. M. El-Chafei, *J. Chem. Soc.*, 1957, 796.
18 R. Sato, T. Nagaoka and M. Saito, *Tetrahedron Lett.*, 1990, **31**, 4165.
19 Preliminary results of the crystal structure of **2** have been previously reported, see references 1 and 3.
20 Y. V. Zefirov, *Crystallogr. Rep.*, 1997, **42**, 111.

21 J. J. P. Stewart, *J. Comput. Chem.*, 1989, **10**, 209.
22 M. J. S. Dewar, E. G. Zoebisch, E. F. Healy and J. J. P. Stewart, *J. Am. Chem. Soc.*, 1985, **107**, 3902.
23 J. J. P. Stewart, *MOPAC 93*; Fujitsu Limited: Tokyo, Japan; all rights reserved.
24 M. J. S. Dewar, E. F. Healy, A. J. Holder and Y.-C. Yuan, *J. Comput. Chem.*, 1990, **11**, 541.
25 J. J. P. Stewart, *J. Comput. Chem.*, 1990, **11**, 543.
26 S. Kammermeier and R. Herges, *Angew. Chem.*, *Int. Ed. Engl.*, 1996, **35**, 417.
27 R. Korenstein, K. A. Muszkat and G. Seger, *J. Chem. Soc.*, *Perkin, Trans. 2*, 1976, 1536.
28 R. Korenstein, K. A. Muszkat and E. Fischer, *J. Chem. Soc.*, *Perkin, Trans. 2*, 1977, 564.
29 M. R. Suissa, PhD Thesis, The Hebrew University of Jerusalem, Jerusalem, 1988.